Supplementary Information

circNDUFB2 inhibits non-small cell lung cancer progression via destabilizing IGF2BPs and activating anti-tumor immunity

Botai Li,[1] Lili Zhu,[1] Chunlai Lu,[1] Liyan Jiang[*] and Wenxin Qin[*]

[1]These authors contributed equally

*Corresponding authors

Supplementary Figure 1

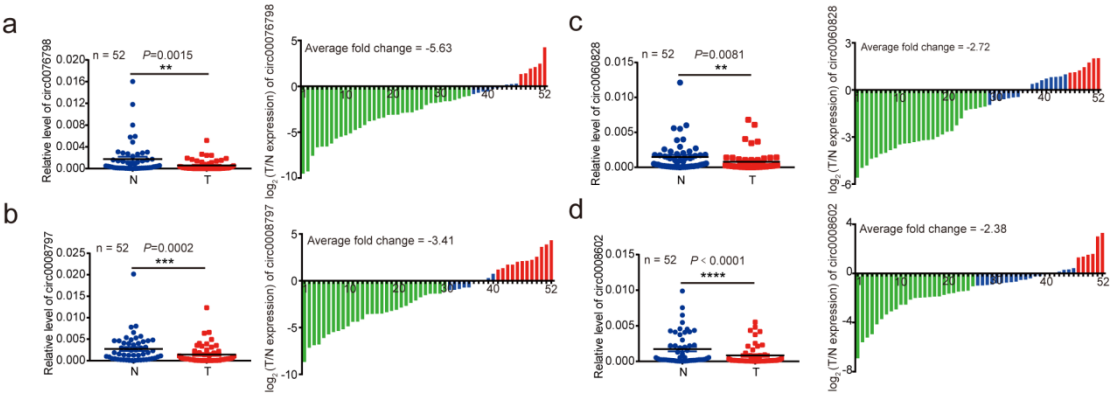

Other four circRNAs remarkably downregulated in NSCLC tissues.

(a-d) Expression levels of the indicated circRNAs in additional 52 paired samples of NSCLC. *GAPDH* was used as the loading control. n=52 biologically independent paired tissues of NSCLC. P values are calculated by paired two-sided t-test in a-d.

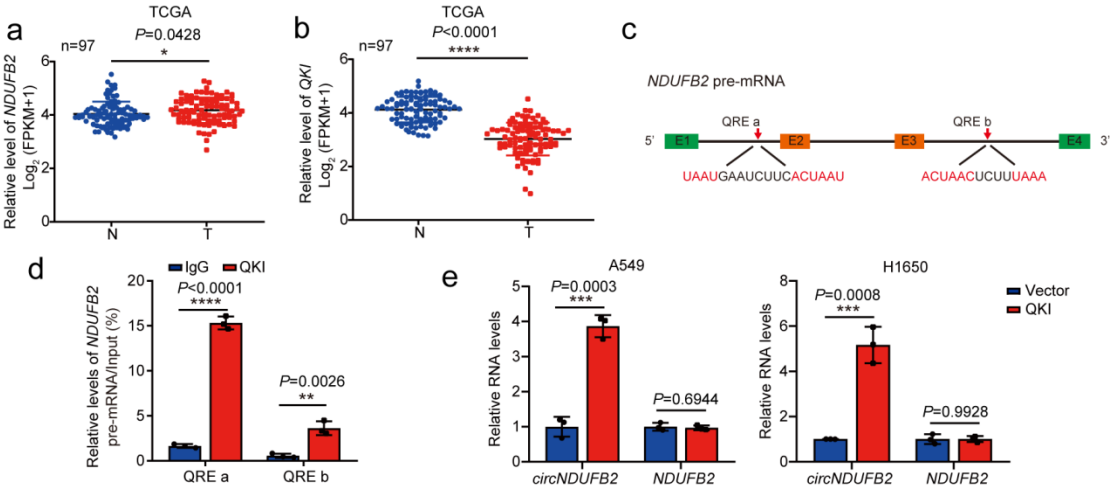

Supplementary Figure 2

QKI promotes *circNDUFB2* formation in NSCLC.

(a-b) mRNA levels of *NDUFB2* (a) and *QKI* (b) for patients with NSCLC in TCGA cohorts. Data are presented as mean ± s.d. P values are calculated by paired two-sided t-test in a-b. n=97 biologically independent paired tissues of NSCLC. (c) A sketch map for potential QRE in the *NDUFB2* pre-mRNA. QRE a and QRE b, two potential QKI response elements in the introns flanking exon 2 and exon 3 of *NDUFB2* pre-mRNA, respectively. (d) Analysis for the *NDUFB2* pre-mRNA enrichment, relative to input. RIP assay was performed using QKI antibody in A549 cells. n=3 biologically independent samples. (e) Expression levels of *circNDUFB2* and *NDUFB2* in A549 and H1650 cells with QKI overexpression. n=3 biologically independent samples. Data are presented as mean ± s.d. P values are calculated by unpaired two-sided t-test in d-e.

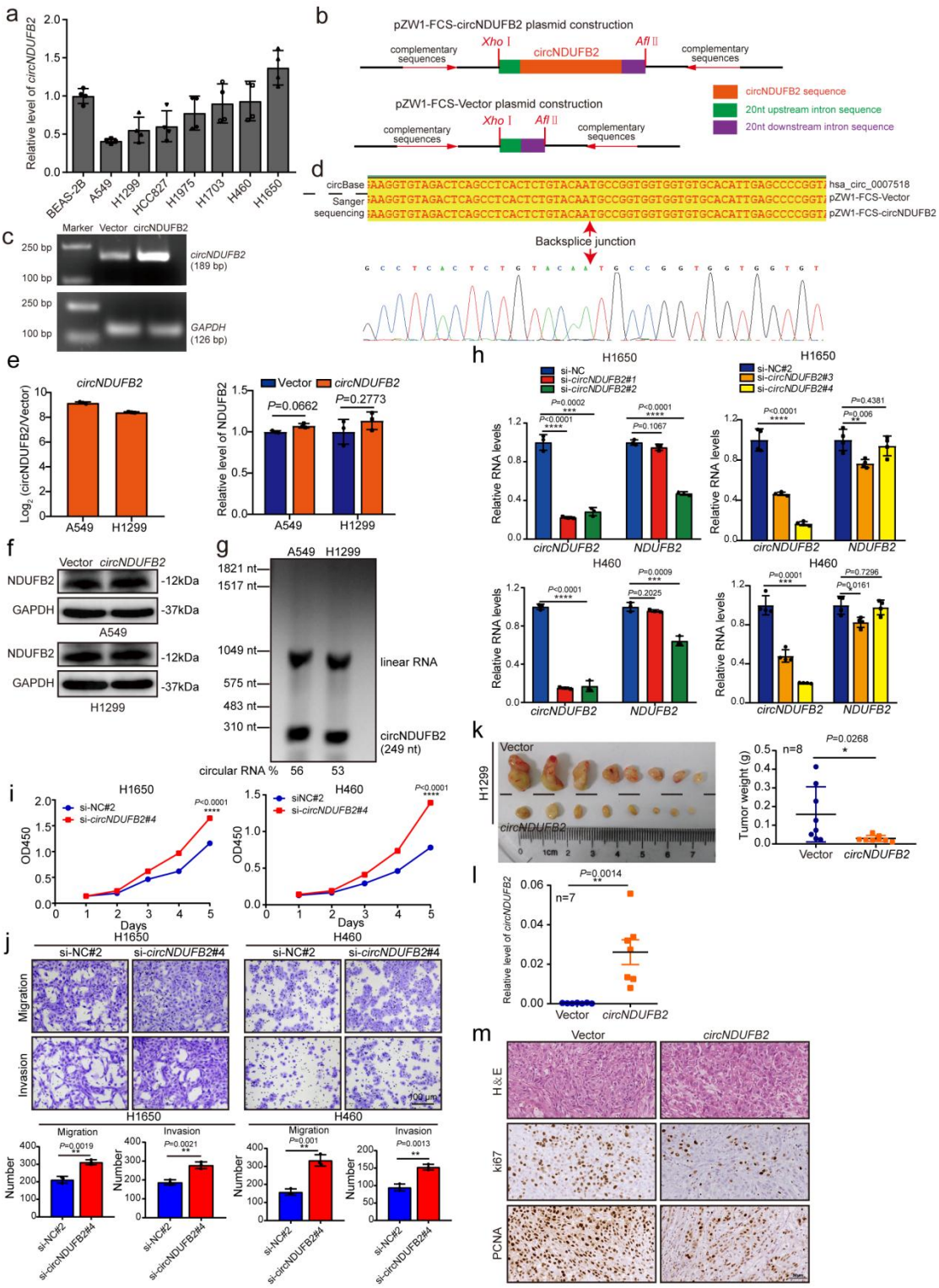

Supplementary Figure 3

Inhibitory effects of *circNDUFB2* on proliferation for NSCLC cells.

(a) Expression levels of *circNDUFB2* in one normal cell line (a human bronchial epithelial cell line BEAS-2B) and seven NSCLC cell lines, relative to BEAS-2B. n=4 biologically independent

samples. (b) A sketch map for plasmid construction of *circNDUFB2* overexpression. (c) PCR analysis for *circNDUFB2* in A549 cells with or without *circNDUFB2* overexpression. (d) Sanger sequencing analysis for PCR products in (c). (e) Expression levels of *circNDUFB2* and *NDUFB2* in NSCLC cells with *circNDUFB2* overexpression. n=3 biologically independent samples. (f) Protein levels of NDUFB2 in NSCLC cells with *circNDUFB2* overexpression. (g) Northern blotting analysis for RNA from A549 cells and H1299 cells transfected with *circNDUFB2* overexpression plasmid. The relative abundance of circular RNA and linear RNA was determined by using the ImageJ program. (h) Expression levels of *circNDUFB2* and *NDUFB2* in NSCLC cells with *circNDUFB2* knockdown. n=3, 3, 4, 4 biologically independent samples, respectively. (i) Cell proliferation assays for NSCLC cells with *circNDUFB2* knockdown. n=5 biologically independent samples. (j) Migration and invasion assays for NSCLC cells with *circNDUFB2* knockdown. n=3 biologically independent samples. Scale bar=100 μm. (k) The weight of subcutaneous xenograft tumors (n=8 mice per group). (l) Expression levels of *circNDUFB2* in subcutaneous xenograft tumors derived from A549 cells. (m) H&E staining and immunohistochemical staining for cell proliferation marker in subcutaneous xenograft tumors derived from A549 cells, scale bar=50 μm. Data are presented as mean ± s.d. P values are calculated by unpaired two-sided t-test in a, e and h-l. Two independent experiments were carried out with similar results in c, f-g and m.

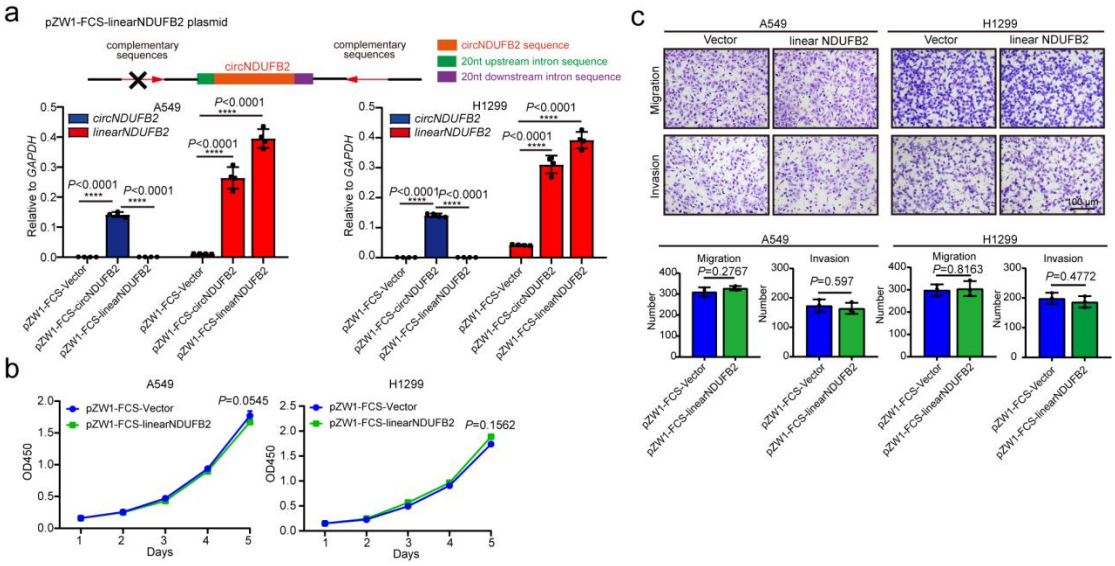

Supplementary Figure 4

Linear-NDUFB2 does not affect NSCLC progression.

(a) Top: A sketch map for pZW1-FCS-linearNDUFB2 plasmid construction. Bottom: qRT-PCR showed pZW1-FCS-circNDUFB2 plasmid produced both *circNDUFB2* and linear-*NDUFB2*, whereas pZW1-FCS-linearNDUFB2 plasmid only produced linear-*NDUFB2*. n=4 biologically independent samples. (b) Cell proliferation assays for NSCLC cells with linear-*NDUFB2* overexpression. n=5 biologically independent samples. (c) Migration and invasion assays for NSCLC cells with linear-*NDUFB2* overexpression. n=3 biologically independent samples. Scale bar=100 μm. Data are presented as mean ± s.d. P values are calculated by unpaired two-sided t-test in a-c.

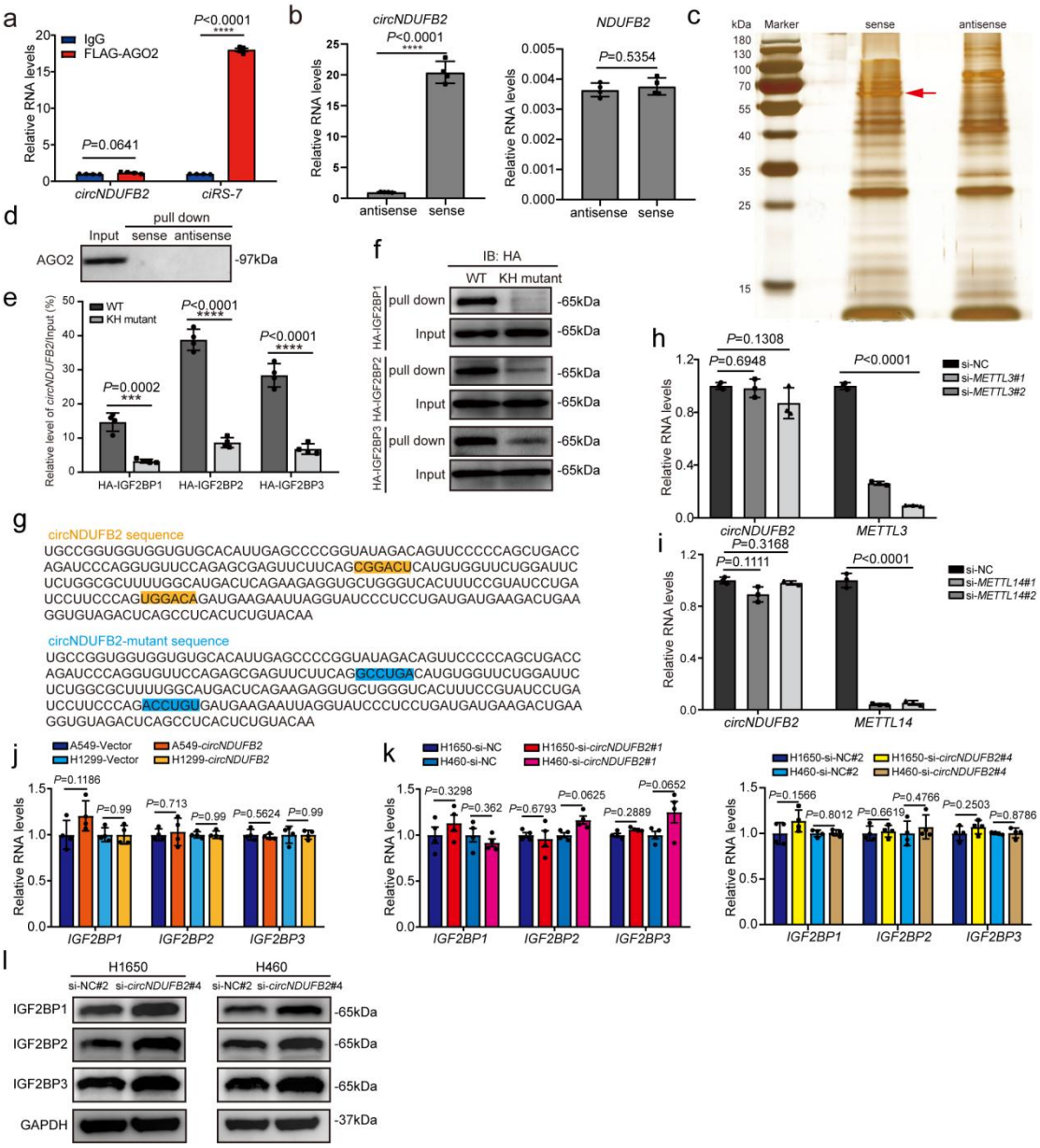

Supplementary Figure 5

circNDUFB2 binds with IGF2BPs.

(a) Analysis for *circNDUFB2* and *ciRS-7* enrichment, relative to IgG. RIP assays were performed using FLAG antibody in A549 cells transfected with FLAG-AGO2 plasmid. n=4 biologically independent samples. (b) Analysis for *NDUFB2* and *circNDUFB2* enrichment. RNA pull down assays were performed using biotinylated sense probe which targets the *circNDUFB2* backsplice junction region. n=4 biologically independent samples. (c) Biotinylated sense probe and antisense

probe were incubated with A549 total cell lysates for RNA pull down assays. After silver staining, the sense-specific band at about 65kDa (red arrow) was excised and analysed using mass spectrometry. (d) RNA pull down showed that *circNDUFB2* didn't interact with AGO2. (e) Analysis for the *circNDUFB2* enrichment, relative to input. RIP assay was performed using HA antibody in the indicated cells. n=4 biologically independent samples. (f) Binding of *circNDUFB2* to IGF2BPs or KH domain mutant IGF2BPs in vitro. (g) Sequences of *circNDUFB2* and *circNDUFB2*-mutant. For the *circNDUFB2*-mutant plasmid, 'CGGACU' was replaced with 'GCCUGA', and 'UGGACA' was replaced with 'ACCUGU', respectively. (h) Expression levels of *METTL3* and *circNDUFB2* in A549 cells with METTL3 knockdown. n=3 biologically independent samples. (i) Expression levels of *METTL14* and *circNDUFB2* in A549 cells with METTL14 knockdown. n=3 biologically independent samples. (j-k) mRNA levels of *IGF2BPs* in NSCLC cells with *circNDUFB2* overexpression (j) or knockdown (k). n=4 biologically independent samples. (l) Protein levels of IGF2BPs in NSCLC cells with *circNDUFB2* knockdown. Data are presented as mean ± s.d. P values are calculated by unpaired two-sided t-test in a-b, e and h-k. Two independent experiments were carried out with similar results in c-d, f and l.

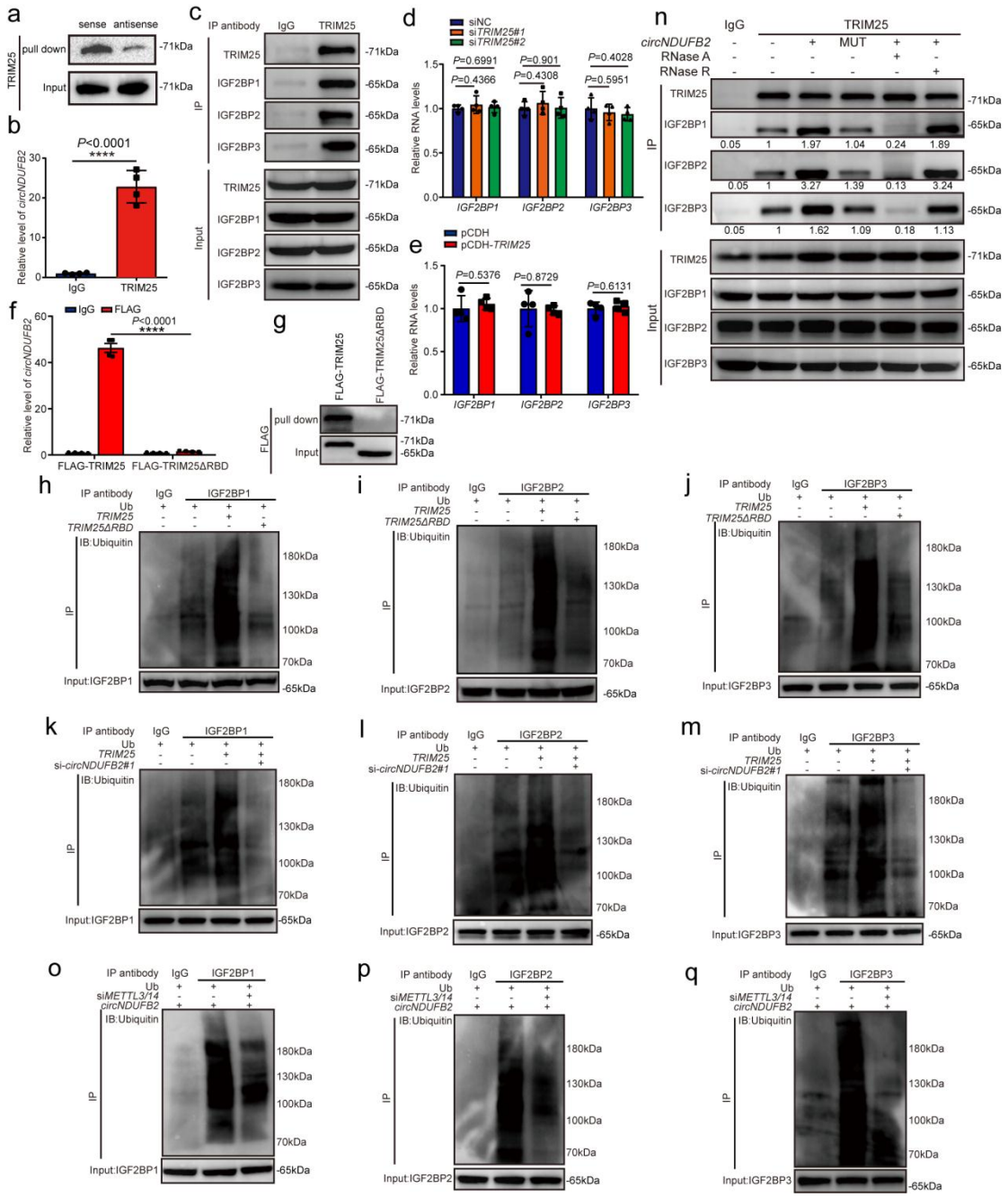

Supplementary Figure 6

TRIM25 promotes ubiquitination and degradation of IGF2BPs in a *circNDUFB2*-dependent manner.

(a) Binding of *circNDUFB2* with TRIM25 in H1299 cells. (b) Analysis for *circNDUFB2* enrichment, relative to IgG. RIP assay was performed using TRIM25 antibody in A549 cells. n=4 biologically independent samples. (c) Co-immunoprecipitation (Co-IP) showed the binding of

TRIM25 with IGF2BPs in A549 cells. (d-e) mRNA levels of *IGF2BPs* in A549 cells with TRIM25 knockdown (d) or overexpression (e), respectively. n=4 biologically independent samples. (f) Analysis for *circNDUFB2* enrichment, relative to IgG. RIP assays were performed using FLAG antibody in A549 cells. n=4 biologically independent samples. (g) RNA pull down assays were performed using biotinylated sense probe for *circNDUFB2* in A549 cells. (h-j) Ubiquitination modification of IGF2BPs in A549 cells transfected with FLAG-TRIM25 or FLAG-TRIM25ΔRBD plasmids. (k-m) Ubiquitination modification of IGF2BPs in A549 cells with TRIM25 overexpression and *circNDUFB2* knockdown. (n) Co-IP showed the binding of TRIM25 with IGF2BP proteins. (o-q) Ubiquitination modification of IGF2BPs in A549 cells with METTL3/14 knockdown. Ub, ubiquitin. Data are presented as mean ± s.d. P values are calculated by unpaired two-sided t-test in b and d-f. Two independent experiments were carried out with similar results in a, c, g and h-q.

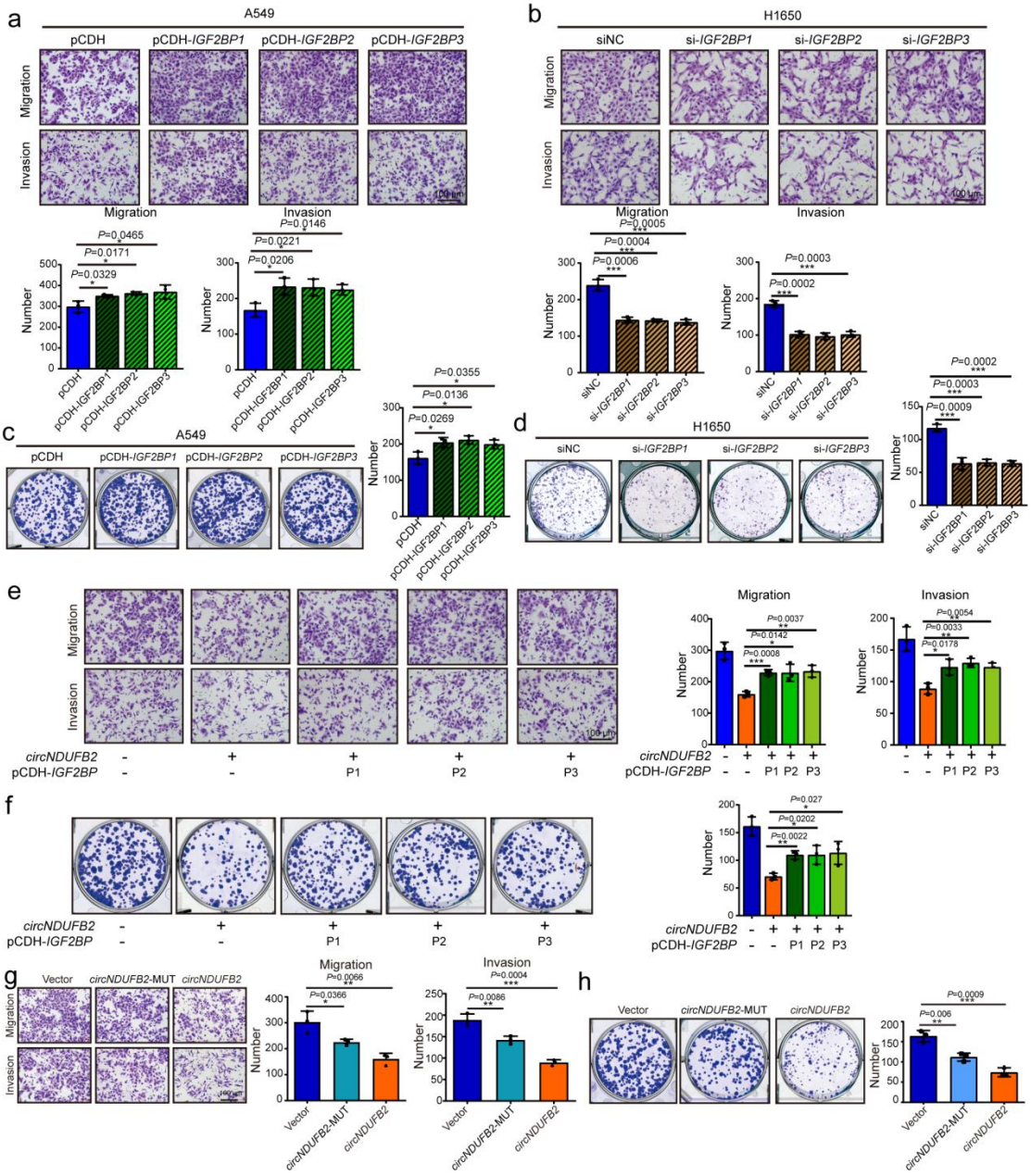

Supplementary Figure 7

IGF2BPs mediate inhibitory effects of *circNDUFB2* on NSCLC progression.

(a-b) Migration and invasion assays for NSCLC cells with IGF2BPs overexpression or knockdown. n=3 biologically independent samples. Scale bar=100 μm. (c-d) Colony formation assays for NSCLC cells with IGF2BPs overexpression or knockdown. n=3 biologically independent samples. (e) Migration and invasion assays showed the restoring effects of IGF2BPs on A549 cells with *circNDUFB2* overexpression. P1, IGF2BP1; P2, IGF2BP2; P3, IGF2BP3. n=3

biologically independent samples. Scale bar=100 μm. (f) Colony formation assays showed the restoring effects of IGF2BPs on A549 cells with *circNDUFB2* overexpression. P1, IGF2BP1; P2, IGF2BP2; P3, IGF2BP3. n=3 biologically independent samples. (g) Migration and invasion assays for A549 cells with overexpression of *circNDUFB2* or *circNDUFB2*-mutant. n=3 biologically independent samples. Scale bar=100 μm. (h) Colony formation assays for A549 cells with overexpression of *circNDUFB2* or *circNDUFB2*-mutant. n=3 biologically independent samples. Data are presented as mean ± s.d. P values are calculated by unpaired two-sided t-test in a-h. Two independent experiments were carried out with similar results in a, b, e and g.

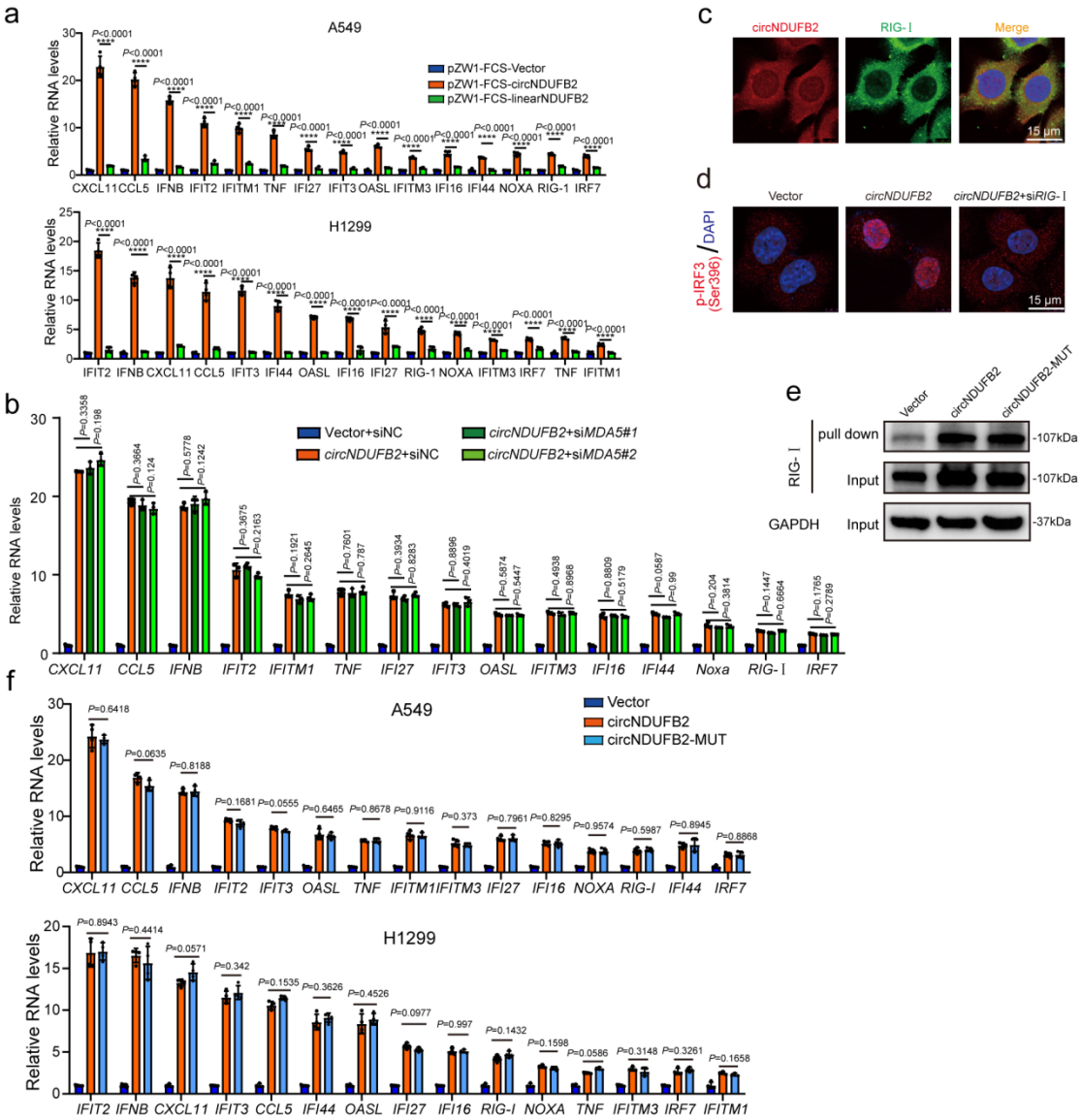

Supplementary Figure 8

circNDUFB2 binds with RIG-I.

(a) Expression levels of indicated mRNA in NSCLC cells with *circNDUFB2* or linear-*NDUFB2* overexpression. n=4 biologically independent samples. (b) Fold change of indicated mRNAs in A549 cells with or without MDA5 knockdown. n=3 biologically independent samples. (c) RNA FISH-immunofluorescence showed the co-localization of *circNDUFB2* (red) with RIG-I (green) in A549 cells. Scale bar=15 μm. (d) Immunofluorescence detected the localization of p-IRF3 in A549 cells. Scale bar=15 μm. (e) RNA pull down assay was performed using biotinylated sense

probe for *circNDUFB2* in A549 cells with *circNDUFB2* or *circNDUFB2*-MUT overexpression. (f) Expression levels of indicated mRNAs in NSCLC cells with *circNDUFB2* or *circNDUFB2* mutant overexpression. n=4 biologically independent samples. Data are presented as mean ± s.d. P values are calculated by unpaired two-sided t-test in a-b and f. Two independent experiments were carried out with similar results in c-e.

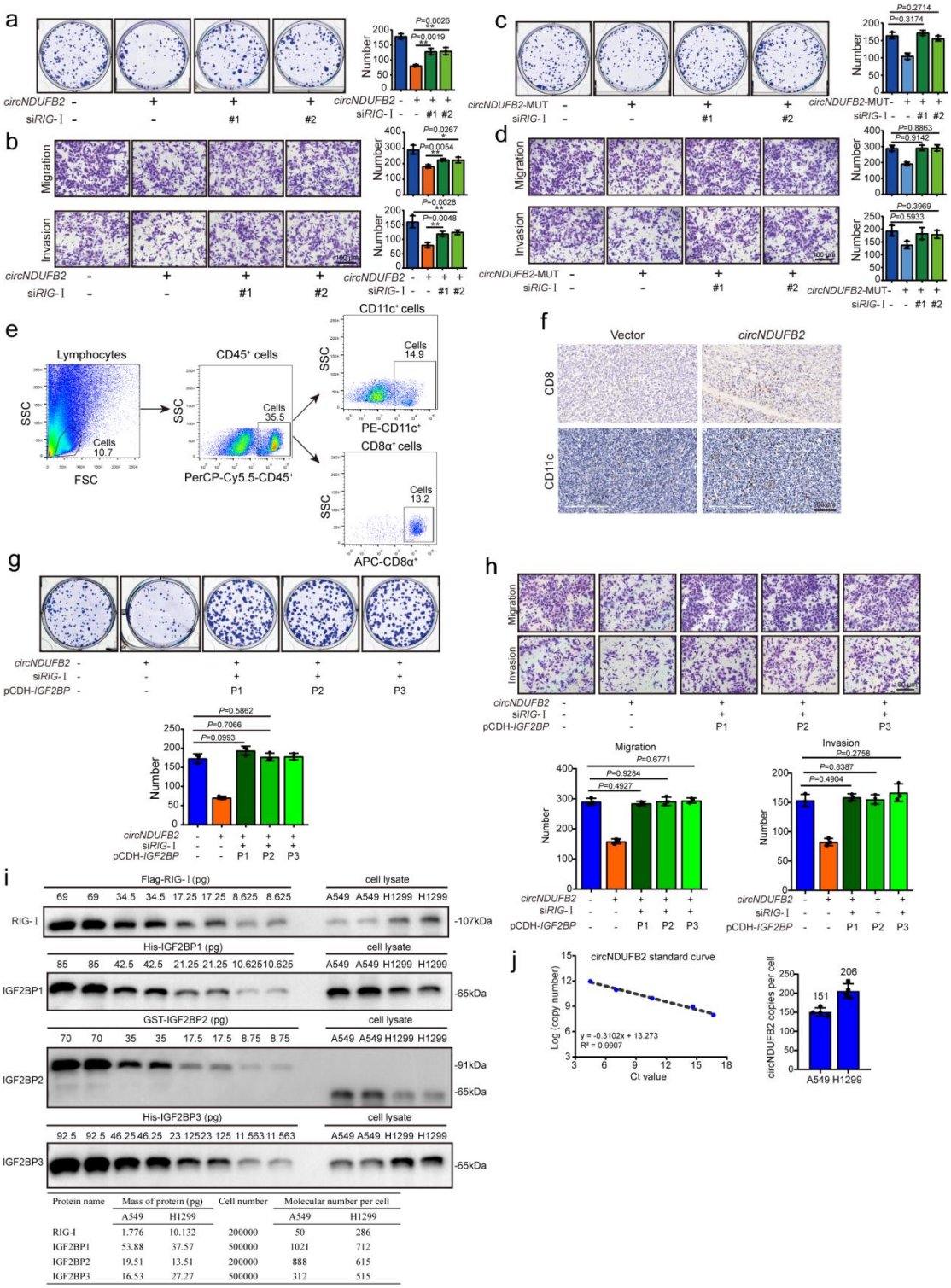

Protein name	Mass of protein (pg)		Cell number	Molecular number per cell	
	A549	H1299		A549	H1299
RIG-I	1.776	10.132	200000	50	286
IGF2BP1	53.88	37.57	500000	1021	712
IGF2BP2	19.51	13.51	200000	888	615
IGF2BP3	16.53	27.27	500000	312	515

Supplementary Figure 9

Immune responses of *circNDUFB2* mediated by RIG-I inhibits tumor progression.

(a-b) Colony formation assays and migration assays showed the restoring effects of RIG-I on A549 cells with *circNDUFB2* overexpression. n=3 biologically independent samples. Scale

bar=100 μm. (c-d) Colony formation assays and migration assays showed the restoring effects of RIG-I on A549 cells with *circNDUFB2*-MUT overexpression. n=3 biologically independent samples. Scale bar=100 μm. (e) Gating strategy and representative flow cytometry plots for the assessment of $CD45^+$, $CD8\alpha^+$ and $CD11c^+$ cells in *circNDUFB2* overexpression and control LLC1 tumors. (f) IHC staining for CD8 and CD11c in subcutaneous xenograft tumors, scale bar=100 μm. (g-h) Colony formation assays and migration assays showed the restoring effects of IGF2BPs and RIG-I on A549 cells with *circNDUFB2* overexpression. n=3 biologically independent samples. Scale bar=100 μm. (i) Measurement of protein molecular number per cell. Top: western blot analysis for purified recombinant protein and cell lysate corresponding to a known number of NSCLC cells. Bottom: quantification summarized in table. Two independent experiments were carried out with similar results. (j) Copy number of *circNDUFB2* in A549 cells and H1299 cells. Left: the linear relationship between the log *circNDUFB2* copy number and its Ct value by qRT-PCR. Right: the average *circNDUFB2* copies per A549 cell and H1299 cell. n=4 biologically independent samples. P1, IGF2BP1; P2, IGF2BP2; P3, IGF2BP3; Data are presented as mean ± s.d. P values are calculated by unpaired two-sided t-test in a-d, g-h and j.

Supplementary Table 1

Associations between *circNDUFB2* and clinicopathologic features in 52 patients with NSCLC

Clinicopathological features	Number of patients	*circNDUFB2*		P value
		Low	High	
Age (y)				0.1259
<60	15	5	10	
≥60	37	21	16	
Gender				0.0922
Male	30	18	12	
Female	22	8	14	
Smoke				0.0714
Smoker	16	11	5	
Nonsmoker	36	15	21	
Tumor size (cm)				0.0337[a]
<3	16	4	12	
≥3	36	22	14	
Lymph node metastasis				0.0226[a]
No	20	6	14	
Yes	32	20	12	
Stage				0.011[a]
Ⅰ+Ⅱ	31	11	20	
Ⅲ+Ⅳ	21	15	6	

The associations between *circNDUFB2* and clinicopathologic features in patients with NSCLC were analyzed. NSCLC, non-small cell lung cancer. The median expression level was used as the cutoff.

[a]P<0.05, which was considered as a significant difference.

Supplementary Table 2

Clinicopathological characteristics of 55 NSCLC patients used in this study

Cases used for Arraystar Human circRNAs Array analysis (n=3)						
Case	Age	Gender	Smoke	Tumor Size (cm)	Lymph node metastasis	Stage
1	64	Male	YES	3.5*2.5*3	YES	ⅠB
2	56	Female	NO	3.5*3*2.5	YES	ⅡA
3	53	female	NO	4*3*2.5	YES	ⅢA

Cases used for qRT-PCR validation (n=52)					
Age (<60:≥60)	Gender (Male:Female)	Smoke (NO:YES)	Tumor size, cm (<3:≥3)	Lymph node metastasis (NO:YES)	Stage (Ⅰ+Ⅱ:Ⅲ+Ⅳ)
15:37	30:22	36:16	14:38	19:33	31:21

Supplementary Table 3

Mass spectrometry identification of proteins pulled down at about 65kDa

Gene name	Protein_score	Protein_coverage	MW [kDa]
IGF2BP2	566	23.2	66.2
IGF2BP1	211	14.7	63.8
IGF2BP3	175	10.5	64
COIL	142	12.7	63.3
HNRNPLL	118	10.7	60.9
NOP56	87	6.2	66.4
CLK2	75	6	60.5
KPNA1	46	3.2	60.9
STAU1	40	2.9	63.4
PUF60	35	1.8	60
CSTF2	34	1	61
DDX56	32	0.9	62
HIRIP3	32	0.9	62.3
KPNA6	30	3	60.7
CSRNP1	30	4.1	64.8
INSM2	26	0.9	60.5
TCP1	26	1.8	60.8
DDX28	25	1.7	59.8
UGT1A7	25	0.9	60.6
RELA	24	1.1	60.7
CRMP1	24	0.9	62.5
CCDC102A	24	1.1	62.8
CPNE3	23	1.7	60.9
ZNF18	23	1.3	63.2
TMEM200C	23	1	64.3
PANK2	21	0.9	63.3

Supplementary Table 4

Antibodies used in this study

Antibodies	Source	Identifier
Anti-AGO2	Abcam	Cat#ab186733
Anti-CD8	Abcam	Cat#ab22378
Anti-IFNβ	Abcam	Cat#ab176343
Anti-ki67	Abcam	Cat#ab16667
Anti-PANA	Abcam	Cat#ab29
Anti-TRIM25	Abcam	Cat#ab88669
Anti-GAPDH	Proteintech	Cat#60004-1-Ig
Anti-HA	Proteintech	Cat#51064-2-AP
Anti-HECTD3	Proteintech	Cat#11487-1-AP
Anti-IGF2BP1	Proteintech	Cat#22803-1-AP
Anti-IGF2BP2	Proteintech	Cat#11601-1-AP
Anti-IGF2BP3	Proteintech	Cat#14642-1-AP
Anti-IRF3	Proteintech	Cat#11312-1-AP
Anti-IRF7	Proteintech	Cat#22392-1-AP
Anti-NDUFB2	Proteintech	Cat#17614-1-AP
Anti-RIG-I	Proteintech	Cat#20566-1-AP
Anti-TNF	Proteintech	Cat#60291-1-Ig
Anti-TRIM25	Proteintech	Cat#12573-1-AP
Anti-Ubiquitin	Proteintech	Cat#10201-2-AP
Anti-CD11C	Cell Signaling Technology	Cat#97585
Anti-P65	Cell Signaling Technology	Cat#8242
Anti-p-P65 (Ser536)	Cell Signaling Technology	Cat#3033
Anti-p-IRF3 (Ser396)	Cell Signaling Technology	Cat#29047
Anti-p-STAT1 (Tyr701)	Cell Signaling Technology	Cat#9167
Anti-p-STAT2 (Tyr690)	Cell Signaling Technology	Cat #88410
Anti-rabbit IgG (H+L), F(ab')2 Fragment (Alexa Fluor® 488 Conjugate)	Cell Signaling Technology	Cat#4412
Anti-rabbit IgG (H+L), F(ab')2 Fragment (Alexa Fluor® 594 Conjugate)	Cell Signaling Technology	Cat#8889
Anti-mouse IgG (H+L), F(ab')2 Fragment (Alexa Fluor® 488 Conjugate)	Cell Signaling Technology	Cat#4408
Anti-CD8α	Biolegend	Cat#100712
Anti-CD11C	Biolegend	Cat#117308
Anti-CD45	Invitrogen	Cat#45-0451-82
Anti-QKI	BETHYL	Cat#A300-183A
Anti-Flag	Sigma	Cat#F1804
Anti-rabbit-IgG-HRP	Bioworld	Cat#BS13278
Anti-mouse-IgG-HRP	Bioworld	Cat#BS12478